



HAL
open science

Effect of Discretization of Permeability Term and Mesh Size on Macro- and Meso-segregation Predictions

Hervé Combeau, Arvind Kumar, Bernard Dussoubs, Miha Založnik

► **To cite this version:**

Hervé Combeau, Arvind Kumar, Bernard Dussoubs, Miha Založnik. Effect of Discretization of Permeability Term and Mesh Size on Macro- and Meso-segregation Predictions. CFM 2009 - 19ème Congrès Français de Mécanique, Aug 2009, Marseille, France. hal-03378597

HAL Id: hal-03378597

<https://hal.science/hal-03378597v1>

Submitted on 14 Oct 2021

HAL is a multi-disciplinary open access archive for the deposit and dissemination of scientific research documents, whether they are published or not. The documents may come from teaching and research institutions in France or abroad, or from public or private research centers.

L'archive ouverte pluridisciplinaire **HAL**, est destinée au dépôt et à la diffusion de documents scientifiques de niveau recherche, publiés ou non, émanant des établissements d'enseignement et de recherche français ou étrangers, des laboratoires publics ou privés.

Effect of Discretization of Permeability Term and Mesh Size on Macro- and Meso-segregation Predictions

A. KUMAR, B. DUSSOUBS, M. ZALOŽNIK AND H. COMBEAU

Institut Jean Lamour, Nancy-Université, Ecole des Mines de Nancy - Parc de Saurupt – F-54042 Nancy Cedex – France

Abstract :

Macro- and meso-segregations correspond to heterogeneities of composition at the scale of a casting. They develop during the solidification. One of the parameters that has an essential effect on these segregations is the mush permeability which varies over a wide range of magnitude. We present simulation results for solidification of Sn-Pb alloy in a two-dimensional cavity. The role of discretization schemes and mesh size on the formation of channel segregates and macrosegregation is discussed.

Key words: Permeability, Macrosegregation, Channel segregation, Mesosegregation, Darcy equation, Interdendritic, Sn-Pb alloys.

1 Introduction

Fluid flow in the mushy zone plays an important role in the formation of macrosegregation in the castings by redistributing the segregated solute elements [1,2] and in some cases forms channel segregates in the mushy zone [2-4]. The formation of channel segregates (also known as mesosegregations) in castings represents a severe form of segregation since the composition and crystalline structure of the solid which ultimately forms within the channels differ significantly from those of the nearby solid regions. In casting they appear as long narrow trails aligned in some preferred direction, with solute concentration greater than that of the surrounding regions. The interdendritic flow in the mushy region leads to perturbations of the growing columnar structure causing instability of the growth front which leads to further instability of the segregation map leading to the formation of channel segregates. The scale of mesosegregation can affect the homogenization of the ingot and its extent in the casting can severely influence the quality of ingots.

Macrosegregation in casting was widely studied using multiscale models consisting of macroscopic models based on mixture theory [1] or volume averaging [5], coupled to models of microsegregation. In these models, the mushy zone is considered as a saturated porous medium with varying permeability and the flow in the mushy zone is governed by the Darcy law. Carman-Kozeny model is generally used to calculate the permeability. The solution procedures of these macroscopic models involve the discretization of the macroscopic conservation equations based most often either on a finite volume formulation [1-5], or on a finite element formulation. One of the parameters that has an essential effect on macrosegregation profiles is the mush permeability. Permeability in the mushy zone for the simplest model is a function of the liquid fraction and of the dendritic arm spacing (DAS). The dependence of permeability on liquid fraction is highly nonlinear, thus a small variation in the liquid fraction can result in large variation of permeability which can significantly affect the flow in the mushy zone and hence the segregation pattern. Within a volume-averaged solidification model the permeability is the principal parameter of the Darcy term, which describes the hydrodynamic drag of the porous mush in the averaged momentum balance equation. In the finite volume formulation the discretization of the momentum balance equation requires an estimation of the volume integral of the Darcy term over the control volume (CV) by applying some discretization scheme. The way this integration is approximated to get the discretized form of the Darcy term can play an important role in the numerical predictions [4,6]. The permeability (K) (a function of the liquid fraction (g)) is known in the CV points. When using staggered pressure-velocity grids the Darcy term has to be integrated over the velocity CV using some interpolation of the permeability from the adjacent pressure CVs. The objective of the present article is to investigate the effect of discretization schemes for permeability term on predictions of macrosegregation and channel segregates in the mushy region.

2 Mathematical modelling

The conservation equations for mass, heat and solute are averaged over both liquid and solid phase (assuming fixed solid phase, equal and constant solid and liquid densities except in the buoyancy term, where Boussinesq approximation is used and Scheil law for microsegregation) and are given as follows [2,4]:

$$\text{Mass conservation:} \quad \nabla \cdot \mathbf{v} = \nabla \cdot (g_1 \mathbf{v}_l) = 0 \quad (1)$$

$$\text{Energy conservation:} \quad \rho \frac{\partial h}{\partial t} + \rho c_p \mathbf{v} \cdot \nabla \mathbf{T} = \nabla \cdot (k \nabla T) \quad (2)$$

where the average enthalpy is expressed as

$$h = g_s h_s + (1 - g_s) h_l = c_p (T - T_0) + (1 - g_s) L \quad (3)$$

$$\text{Solute conservation:} \quad \rho \frac{\partial C}{\partial t} + \rho \mathbf{v} \cdot \nabla C_1 = 0 \quad (4)$$

Due to the small diffusion coefficient, the diffusion term is neglected in equation (4).

Momentum conservation for the liquid phase:

$$\rho \frac{\partial \mathbf{v}}{\partial t} + \frac{\rho}{g_1} \mathbf{v} \cdot (\nabla \mathbf{v}) = \mu \nabla^2 \mathbf{v} - g_1 \frac{\mu}{K} \mathbf{v} + \rho_0 [\beta_T (T - T_0) + \beta_c (C_1 - C_0)] g_1 \mathbf{g} - g_1 \nabla p \quad (5)$$

The mushy zone is a porous medium saturated with liquid whose permeability is defined through Carman-Kozeny relation.

$$K = \frac{\lambda_2^2 g_1^3}{180(1 - g_1)^2} \quad (6)$$

The term $g_1 \frac{\mu}{K} \mathbf{v}$ corresponds to a drag force of the solid skeleton on the interdendritic liquid region. In the present work the focus is on the evaluation of this term using different discretization schemes. The governing transport equations have been solved using the finite volume technique [7]. All scalar variables (enthalpy, temperature, pressure, etc.) are computed at the centre of the pressure CVs, while a staggered grid is used to determine the components of the velocity at the faces of the pressure CVs. The SIMPLEC algorithm is used to treat the pressure-velocity coupling. A specific algorithm, detailed in [2] has been implemented in order to resolve the non linearity of the transport equations, and in particular the relationship between temperature and enthalpy.

2.1 Discretization of the permeability term

In the mushy zone the only significant forces of the momentum balance are the Darcy drag, the pressure gradient and the buoyancy. This reduces the momentum equation (5) to

$$-\frac{\mu}{K} \mathbf{v} + \rho_0 [\beta_T (T - T_0) + \beta_c (C_1 - C_0)] g_1 \mathbf{g} - \nabla p = 0 \quad (7)$$

Due to the strong nonlinear dependence of the permeability K on the liquid fraction g_1 the discretization of the Darcy term is critical for the accuracy of the numerical solution of the flow in the mushy zone. To get the discretized form of this term we have to approximate its integral across the control volume $\int_V \frac{\mu}{K} \mathbf{v} dV$. For the

horizontal component of the momentum equation this means integration between the faces 'w' and 'e' of the velocity CV 'P', which corresponds to the adjacent pressure points. This gives $\int_w^e \frac{\mu}{K} v_x S dx$, where S is the

cross section of the CV. We point out that in all schemes we approximate the velocity to be constant across the whole velocity CV. With constant viscosity the integral is evaluated as

$$\int_w^e \frac{\mu}{K} v_x S dx = \mu v_{x,P} S \int_w^e \frac{dx}{K} = \mu v_{x,P} S \frac{1}{\bar{K}_P} \quad (8)$$

where \bar{K}_P is the effective discretized value of the permeability in CV 'P' that is evaluated using an approximation of the integral $\int_w^e \frac{dx}{K}$ by some interpolation of K between the faces 'w' and 'e', where it is

known. We now introduce four different discretization schemes for the approximation of this integral using different ways of interpolating K between the two adjacent pressure points.

(a) Linear interpolation of the permeability between two adjacent cells.

- (b) Harmonic mean of the permeability between two adjacent cells.
- (c) Volume weighted interpolation of the liquid fraction between two adjacent cells and computation of the permeability with the interpolated value of the liquid fraction.
- (d) Analytical integration of the Darcy term assuming a linear variation of g_l between the adjacent pressure points.

$$\frac{1}{\bar{K}_p} = \int_w^e \frac{dx}{K(g_l(x))} \quad (9)$$

The dependence of the permeability on the liquid fraction $K(g_l)$ is given by Eq. (6) and the variation of the liquid fraction $g_l(x)$ is assumed to be linear between the adjacent pressure points ‘w’ and ‘e’.

3 Results and discussion

We performed simulations for solidification of a Sn-5 wt %Pb binary alloy in a 2D rectangular cavity (the well-known benchmark experiment by Hebditch and Hunt [8], see FIG. 1). The cavity is cooled from the left side (a constant heat transfer coefficient and a constant coolant temperature) and the remaining three sides are thermally insulated. The thermophysical property data, boundary conditions and parameters used in the computations are reported in [4]. For the present alloy the thermal and solutal buoyancy are cooperating as the heavier solute (Pb) is rejected into the liquid upon solidification. This thermosolutal configuration tends to create a downward (counter-clockwise) flow in the melt at the cooled side on account of density variations across the phase changing front.

3.1 Macro- and meso-segregation: Effect of discretization schemes

Figure 2 shows segregation maps in the cavity obtained with different discretization schemes and on a regular 60×60 mesh. For all segregation maps (FIGS. 2a-d), it is observed that the rejected solute-rich liquid flowing towards the bottom of the rectangular cavity in the mushy zone by the counter-clockwise thermo-solutal convection results in patches of thin structure in the mushy zone. These patches in the solute field are known as channel segregates which is a severe form of segregation on an intermediate scale (also referred to as mesosegregation). These channels are formed by perturbation in the mushy zone by the interdendritic fluid flow and in some cases by the localized remelting in some portions of the mush/melt interface. The segregated channels in the bottom of the cavity cover approximately two-thirds of the ingot length.

In a recent study [4] on application of different discretization schemes to simplified a 1D problem, it has been shown that the harmonic mean solution underestimates the predictions whereas solution using interpolated liquid fraction overestimates it. Linear interpolation of permeability shows largest deviation from the exact solution and seems to be the worst discretization scheme and schemes using either the analytical integration or interpolated liquid fraction produce results closer to the exact solution. In present simulations also results obtained with the linear interpolation scheme (FIG. 2d) are the farthest from the result obtained using the analytical integration scheme. When using linear interpolation of permeability, one can note that (1) the number of channels has decreased from 10 to 8, (2) the nature of these channels is completely different compared to the solution using other three discretization schemes, and (3) the macrosegregation map is also different which has also an effect on the intensity of positive segregation towards the right wall of the cavity. Results using the other schemes (analytical integration scheme, discretization using interpolated liquid fraction and harmonic mean scheme) remain in the same range. However, among the three discretization schemes, prediction of channel segregates using analytical integration scheme and interpolated liquid fraction (FIG. 2a and 2c) are closer to each other and channel segregates obtained using harmonic mean scheme (FIG. 2b) are slightly different and are comparatively less pronounced. We can see that with the analytical integration scheme, the extent of some of the channels is more penetrated into the mushy region compared to the harmonic interpolation. It seems that more penetrated channels are the direct consequence of the relatively higher velocity obtained with the analytical integration scheme, compared to the harmonic interpolation [4].

We found that different discretization schemes give rise to different velocities in the mushy region and hence different nature of segregated channels. For coarser mesh (say 60×60 nodes) discretization of permeability using interpolated liquid fraction or analytical integration seems to produce similar results. However, results with harmonic mean interpolation differ from these two and linear interpolation gives completely different results.

3.2 Mesosegregation: Effect of mesh size

It has been reported in ref. [4] that when the number of nodes is increased, the discretization error of all solutions decreases to reasonable values, as they all converge to the exact solution. For industrial ingots, the number of cells in the mushy region is generally ~ 10 , for which there could be large differences in the solutions obtained using different discretization schemes, and therefore appropriate care has to be taken for discretization of the permeability when not using very fine mesh [4]. For 60×60 mesh we saw that prediction of channel segregates using linear interpolation is far different from the analytical integration and interpolated liquid fraction scheme. For that, the linear interpolation scheme is completely discarded for discretizing the permeability term. Predictions using interpolated liquid fraction and analytical integration schemes are closer to each other; however, predictions using harmonic mean are again slightly different from prediction using these two. To study the sensitivity of such differences with mesh size used in computations, we performed simulations with finer mesh for two schemes, namely analytical integration and harmonic interpolation. Figure 3 shows that with refinement of grids the difference between the predictions using these two schemes vanishes.

The dependence on mesh size is far greater than that on discretization schemes (for instance see results with 90×90 mesh, 150×150 mesh and 300×300 mesh in FIG. 3). A very fine mesh shows a smaller number of channels which are merged with the horizontal channel at the bottom. For fine mesh, mesosegregation is more continuous in the bottom region (i.e. channels connected to the bottom channel). The number and orientation of channels changes with the mesh size as these channels are result of instability occurring in the mushy zone due to variation of local flow conditions. The other observation with fine mesh is disappearance of channels from the middle of the cavity, however, some new channels form towards the bottom left corner of the cavity.

Figure 4 shows the flow pattern in the cavity. In contrast to channel segregates obtained using finer grids (150×150 mesh and 300×300 mesh), the relatively coarse grid solution (90×90 mesh) shows that the local fluid flow crosses the channel. In finer grid solution (150×150 mesh and 300×300 mesh), most of the flow enters the channel from above and due to the smaller flow resistance follows the channel, which drives its growth. As seen in FIG. 3, with finer grids the channels merge with the horizontal channel at the bottom. This is due to a new organization of local fluid flow with a preferential path along the channel (see FIG. 4) which drives its growth and merges the channels to the bottom channel making them more continuous in the bottom region. For the same new organization of fluid flow along some preferential path, channels from the middle of the cavity disappear and some new channels form towards the lower left corner of the cavity. This can be clearly seen in FIG. 4 (for 300×300 mesh) where the local fluid flow in the middle of the cavity is across the cavity, however, in the channels and lower left corner it has a preferential path.

With relatively coarse grid most of the flow crosses the channel trying to tilt the channel towards bottom. With finer grids most of the flow is within the channel which drives its growth. This explains the different inclinations of channels obtained using various nodes. With finer grids since the channels have been captured with more than one point along their width, we start to resolve the flow within the channel. This allows the determination of the channel width. In the present study, for the first time, the size of the channel has been determined. The width of the channel for various mesh size viz. 90×90 mesh, 150×150 mesh and 300×300 mesh are $1685 \mu\text{m}$, $1550 \mu\text{m}$ and $1000 \mu\text{m}$, respectively.

4 Conclusions

The present 2D simulations show that result with interpolated liquid fraction scheme and analytical integration scheme are similar. For the simulation with relatively coarser mesh, say for industrial ingot, discretization of permeability using interpolated liquid fraction scheme and analytical integration scheme is advisable. However, with finer grids any discretization scheme produces similar results. We found that mesh refinement is crucial to capture the complex phenomena occurring in the case of formation of channel segregates. An important conclusion is that a coarse mesh can capture rather well the risk to form mesosegregations, but only a fine mesh is able to resolve the complex phenomena involved in more detail. With a very fine mesh, channels have been captured with more than one point along their width, allowing the determination of the channel width. In the present study, for the first time, the size of the channel has been determined.

Acknowledgements

This work has been performed in the frame of the project 'SMACS' N°BLAN07-2_193017 financed by ANR.

References

- [1] Prakash C. and Voller V.R., Numer. Heat Transfer B, 15, 171-189, 1989.
- [2] Ahmad N., Combeau H., Desbiolles J.-L., Jalanti T., Lesoult G., Rappaz J., Rappaz M. and Stomp C., Metall. Mater. Trans., 29A, 617-630, 1998.
- [3] Combeau H., Založnik M., Hans S., and Richy P.E., Metall. and Mater. Trans. B, in press, DOI: 10.1007/s11663-008-9178-y, 2008.
- [4] Kumar A., Dussoubs B., Založnik M. and Combeau H., J. Phys. D: Appl. Phys. Accepted
- [5] Ni J. and Beckermann C., Metall. and Mater. Trans. B, 22B, 349-361, 1991.
- [6] Katz R.F. and Worster M.G., J. Computational Phys., 227, 9823-9840, 2008.
- [7] Patankar S.V., Numerical Heat Transfer and Fluid Flow, Hemisphere Publication, Washington D.C., 1980.
- [8] Hebditch D. and Hunt J., Metall. Trans., 5, 1557-1564, 1974.

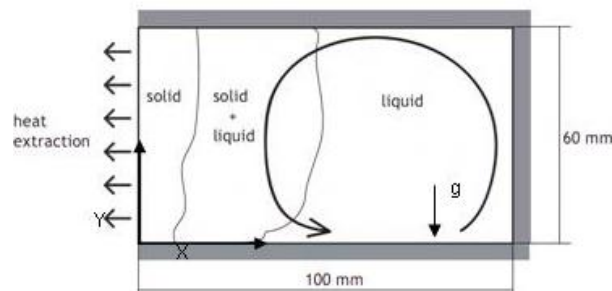


FIG. 1 - Schematic of the 2D side-cooled solidification problem

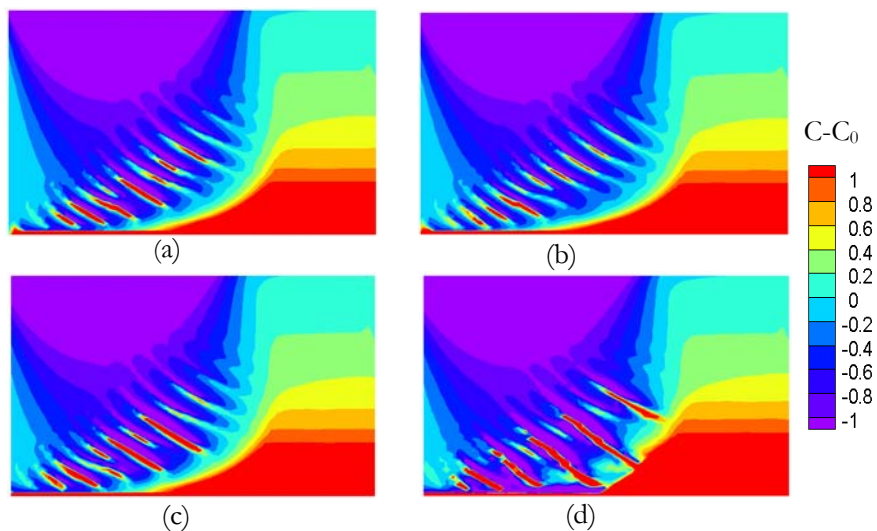


FIG. 2 - Macrosegregation map at $t=400s$ (60×60 mesh): (a) analytical discretization of permeability; (b) harmonic interpolation of permeability; (c) permeability evaluation using interpolated liquid fraction; (d) linear interpolation of permeability

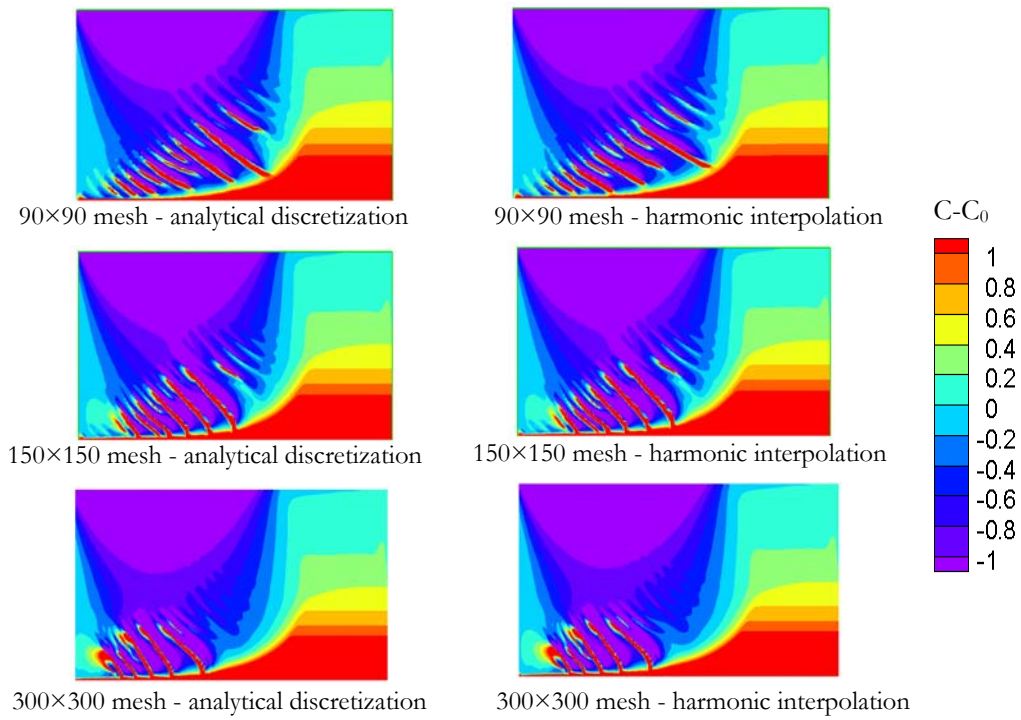


FIG. 3 - Macrosegregation map at $t = 400$ s for different mesh size

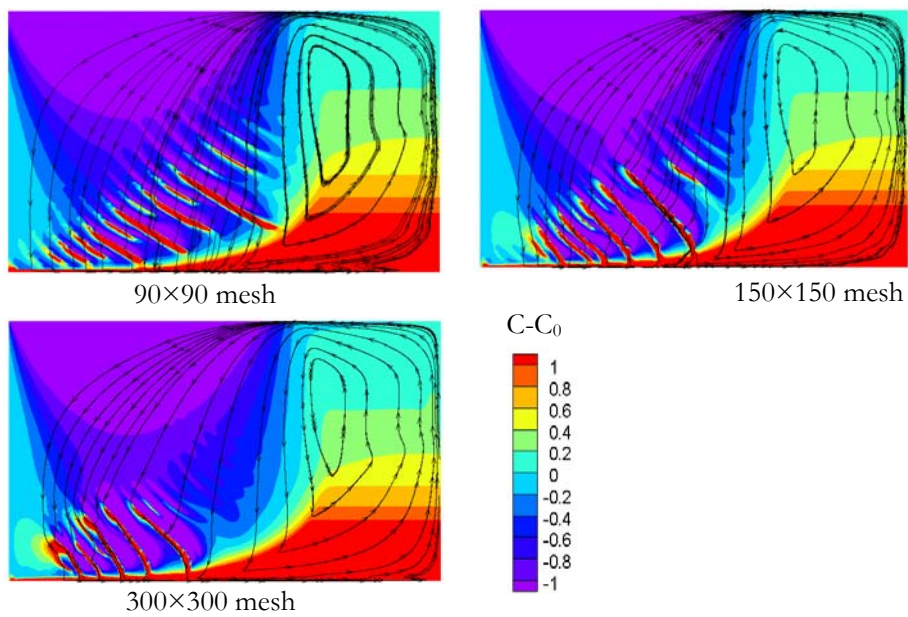


FIG. 4 - Flow field (shown by streamlines) and macrosegregation (shown by colour scale) at $t = 400$ s for the harmonic interpolation scheme.